Water Research 229 (2023) 119437

Contents lists available at ScienceDirect

Water Research

journal homepage: www.elsevier.com/locate/watres

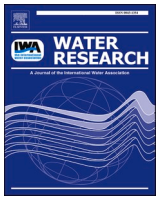

Waterborne virus transport and the associated risks in a large lake

Chaojie Li [a], Émile Sylvestre [b], Xavier Fernandez-Cassi [a,1], Timothy R. Julian [b,c,d], Tamar Kohn [a,*]

[a] Laboratory of Environmental Chemistry, School of Architecture, Civil and Environmental Engineering, (ENAC), École Polytechnique Fédérale de Lausanne, Lausanne, Switzerland
[b] Department Environmental Microbiology, Eawag-Swiss Federal Institute of Aquatic Science and Technology, Dübendorf, Switzerland
[c] Swiss Tropical and Public Health Institute, Basel, Switzerland
[d] University of Basel, Basel, Switzerland

ARTICLE INFO

Keywords:
Water quality simulation
Waterborne virus inactivation
Risk assessment
Human health

ABSTRACT

Waterborne enteric viruses in lakes, especially at recreational water sites, may have a negative impact on human health. However, their fate and transport in lakes are poorly understood. In this study, we propose a coupled water quality and quantitative microbial risk assessment (QMRA) model to study the transport, fate and infection risk of four common waterborne viruses (adenovirus, enterovirus, norovirus and rotavirus), using Lake Geneva as a study site. The measured virus load in raw sewage entering the lake was used as the source term in the water quality simulations for a hypothetical scenario of discharging raw wastewater at the lake surface. After discharge into the lake, virus inactivation was modeled as a function of water temperature and solar irradiance that varied both spatially and temporally during transport throughout the lake. Finally, the probability of infection, while swimming at a popular beach, was quantified and compared among the four viruses. Norovirus was found to be the most abundant virus that causes an infection probability that is at least 10 times greater than the other viruses studied. Furthermore, environmental inactivation was found to be an essential determinant in the infection risks posed by viruses to recreational water users. We determined that infection risks by enterovirus and rotavirus could be up to 1000 times lower when virus inactivation by environmental stressors was accounted for compared with the scenarios considering hydrodynamic transport only. Finally, the model highlighted the role of the wind field in conveying the contamination plume and hence in determining infection probability. Our simulations revealed that for beaches located west of the sewage discharge, the infection probability under eastward wind was 43% lower than that under westward wind conditions. This study highlights the potential of combining water quality simulation and virus-specific risk assessment for a safe water resources usage and management.

1. Introduction

Human enteric viruses are frequent contaminants of recreational water (Aslan et al., 2011; Brouwer et al., 2018; Corsi et al., 2016) and have been found to cause disease outbreaks (Cabelli, 1983; Sinclair et al., 2009). Yet, viral contamination in recreational waters is rarely directly monitored, because traditional culturing assays are time consuming and molecular techniques tend to overestimate the infectious virus concentrations in a sample (Farkas et al., 2020). Instead, the microbial quality of surface water is often assessed by monitoring fecal indicator bacteria, such as *E. coli* (WHO Scientific Group, 1979), which are much easier to measure. Although previous studies of waterborne diseases outbreaks showed that bacteriological indicators are typically present when viral outbreaks occur, the occurrence of fecal coliforms in recreational water sites does not necessarily indicate viral pollution (Sinclair et al., 2009). Thus, it is critical to specifically consider viral pathogens when assessing the risk of infection during recreational water use. Nevertheless, viral pathogens are typically not included in water quality monitoring programs (Boehm et al., 2009; WHO, 2021). Although progress has been made in detecting enteric viruses in recreational water samples using PCR-based molecular methods, the temporal resolution of such measurements is limited due to the cost and complexity of the methods and the requirement of proficient expertise to perform the measurements (Tong et al., 2011). Adding to the complexity of monitoring efforts is environmental virus inactivation, which is an important factor limiting the infectious virus concentration in the

* Corresponding author.
E-mail address: tamar.kohn@epfl.ch (T. Kohn).
[1] Present address: Faculty of Pharmacy and Food Sciences, Universitat de Barcelona, Barcelona, Spain.

https://doi.org/10.1016/j.watres.2022.119437
Received 24 August 2022; Received in revised form 4 November 2022; Accepted 26 November 2022
Available online 28 November 2022

environment (Boehm et al., 2018). If the source of contamination is located at a distance from the monitoring site and the polluted water has aged, the virus concentration measured by molecular methods may greatly overestimate the infectious concentration (Hamza et al., 2011).

Despite the challenges in monitoring waterborne pathogen contamination in natural water bodies, scientists have long endeavored to understand the emergence and transport of pathogens in aquatic systems. Documented studies of waterborne pathogens in lakes trace back to the early 20th century (McLaughlin, 1912). Entering the 21st century, the concept of modeling rather than monitoring pathogen concentrations in lakes started to gain popularity. Modeling approaches offer opportunities for insight into pathogen concentrations at monitoring sites without the needs for frequent measurements. Numerical models have the potential to provide continuous information in space and time, and three-dimensional analysis is usually more accessible compared to monitoring methods. Among different approaches, water quality models appear particularly suited to deal with virus transport effectively. One reason is that a key factor determining the fate of viruses in the environment, the inactivation of viruses, which varies according to specific environmental conditions, can be readily included in water quality models (Schijven et al., 2015). The study of virus inactivation itself is therefore a crucial topic. A meta-analysis method to estimate the inactivation rate of different viruses as a function of water temperature, solar irradiation, virus species and various other parameters was recently put forward by Boehm et al. (2019), based on a systematic review of measured virus inactivation rates in surface waters. Nevertheless, to the best of our knowledge, this information has not yet been utilized to establish water quality models dedicated to the simulation of waterborne viruses in lakes. Water quality models that neglect impacts of virus inactivation fail to capture attenuation of risks due to spatial heterogeneity in transport.

Most water quality models have been applied to non-viral pathogens in lakes. For example, Hipsey et al. (2004) suggested a three dimensional model to predict *Cryptosporidium parvum* oocyst dynamics in lakes and reservoirs. A few years later, these authors proposed a comprehensive process-based model to address the issue of microbial pollution in aquatic systems (Hipsey et al., 2008), though simulations for viral pathogens were lacking. Later studies coupled hydrodynamic models and microbial transport simulation for fecal indicator bacteria and *Cryptosporidium* spp (Eregno et al., 2016; Tolouei et al., 2019), however, inactivation was either omitted or simply modeled as a constant value. The results were furthermore coupled with a Quantitative Microbial Risk Assessment (QMRA). These studies thus assessed not only the fate and transport of pathogens in lakes but also the resulting risk of human infection. Apart from studies employing mechanistic models, studies applying analytical, regression or Bayesian network approaches also demonstrated capability in predicting water quality conditions (Rigosi et al., 2015; Searcy et al., 2018; Trung Thanh et al., 2021; Wong et al., 2009).

Compared with bacterial or protistean pathogens, less attention has been dedicated to simulating the risks posed by viruses in recreational water sites even though the health risks cause by viruses can outweigh those caused by bacteria (Viau et al., 2011). One study specifically addressing risks resulting from viral contamination was performed by Foreman et al. (2015), who proposed a coupled hydrodynamic, virus inactivation and risk model dedicated to the study of infectious hematopoietic necrosis virus, a fish virus that infects salmon and trout and causes important losses in fish farm industry. However, while these authors did consider virus inactivation, the model did not account for temperature-dependence of this process. A similar approach was also used by Sokolova et al. (2015) to estimate the infection risk for human norovirus, however, this study focused on drinking water safety, and virus inactivation was not considered. A comprehensive tool to estimate microbial contamination based on a surface water quality model in combination with QMRA was proposed by Schijven et al. (2015). This tool, which was intended for rivers, included thermal virus inactivation, but not solar inactivation.

A study focusing specifically on the health risks exerted by different human viruses in lakes is imperative yet lacking. Models of health risks associated with human viral pathogens in lakes would aid policy decisions designed to reduce transmission. In this work, we propose a combined water quality and quantitative microbial risk assessment model to comprehensively study the transport, fate and infection risk of four major human waterborne viral pathogens arising from wastewater discharge into a large lake. We specifically focus on how environmental virus inactivation affects the risks at recreational water sites, and we compare the risk levels of the different viruses included. We use Lake Geneva, located on the border of Switzerland and France, as a study site. Lake Geneva has a surface area of 580 km^2 and volume of 89 km^3, with a maximum depth of ~310 m. It is used as a recreational site and as a drinking water source by more than 800,000 people, and it also receives the discharge of several wastewater treatment plants. Our target virus species include adenovirus, enterovirus, norovirus and rotavirus. These viruses are frequently detected in sewage (Gholipour et al., 2022; Lodder and De Roda Husman, 2005) and are classified to have a moderate to high health significance (WHO, 2011).We incorporate spatially and temporally varying inactivation rates of these viruses in our module dedicated to virus simulations, and we compute the risk of infection to swimmers at a popular recreational site at the shore of Lake Geneva for a hypothetical scenario of discharging raw wastewater at the surface of the lake.

2. Material and methods

2.1. Hydrodynamic modeling

Delft3D, an open source three-dimensional (3D) hydrodynamic and water quality simulation software (https://oss.deltares.nl/web/delft3d), was employed to perform numerical simulations in the shore–region of Lake Geneva. Both the hydrodynamic flow and the water quality (DWAQ) modules were used. The flow model in Delft3D solves the shallow water equations as well as the transport equations in 3D (Deltares, 2015), while the water quality module computes solute transport under a Eulerian framework, directly coupled to the hydrodynamic module. The hydrodynamic model, with 100 layers in the vertical direction using the Z-layer gridding system, a horizontal grid resolution of around 400 m and a time step of 1 min, has been fully calibrated and validated (Baracchini et al., 2020a). We employed the result of the hydrodynamic model which has been placed on an online simulation platform for Lake Geneva (http://meteolakes.ch/; Baracchini et al., 2020b). Meteorological conditions such as wind direction, solar radiation, humidity and temperature were included as driving forces. The water quality model based on a Lagrangian framework was validated in a previous study (Li et al., 2022). Here, we used the equivalent water quality model with identical dispersion coefficients, though in a Eulerian framework.

2.2. Virus inactivation modeling

Virus inactivation was modeled using the water quality module of Delft3D, directly coupled to the hydrodynamic module from Meteolakes. Each virus species was regarded as a degradable tracer in this module. The transport of viruses was passive and governed by the flow of the hydrodynamic module, whereas the inactivation of each viral species was specifically defined in each grid cell according to the approach proposed by Boehm et al. (2019):

$$log_{10}k = \beta_0 + \sum_{i=1}^{n} \beta_i x_i + \varepsilon \quad (1)$$

Where k is the first-order inactivation rate constant (day^{-1}) for a given viral species, β_0 represents the model estimate for background

inactivation (likely chemical and microbial processes) under reference conditions (in darkness at 15 ℃), β_i represents the coefficient for each of the model variables x_i (temperature (T-15 ℃) and irradiance (I)) and ε is a Gaussian white noise term representing the error. In this study, we included two inactivation processes, namely thermal ($\beta_{temp} * (T - 15°C)$ and solar inactivation ($\beta_{solar} * I$). Note that "thermal" inactivation may include both direct and indirect (e.g., driven by temperature-mediated changes in microbial grazing) effects of water temperature on virus inactivation. Compared to the model by Boehm et al. (2019), the contribution of solar radiation was further refined. While Boehm et al. (2019) modeled the contribution of solar inactivation as a binary value that depends solely on the presence or absence of sunlight, we accounted here for daily cloud coverage and solar radiation conditions in Lake Geneva and modeled the solar inactivation as a continuous variable. Specifically, we scaled the coefficients β_{solar}, reported by Boehm et al. (2019) according to differences in irradiance observed throughout the year. Hereby the reported value of β_{solar} was assumed to represent irradiance conditions consistent with those observed on average during the month of August 2019 (highest average monthly irradiance in 2019). The coefficients for other irradiance conditions were scaled linearly according to the value of the solar radiation measured. To this end, we used daily ground-level radiation data for the Lake Geneva region provided by MeteoSwiss (https://www.meteoswiss.admin.ch/). MeteoSwiss reports only global irradiance data, whereas direct solar inactivation of enteric viruses depends mainly on the UVB range of 280–320 nm (Nelson et al., 2018). Here we assumed that the UVB range scales linearly with the global irradiance. Finally, we also considered that the solar inactivation is a depth-dependent process, because lake water readily attenuates light in the UVB region. The irradiance (I_z) at each depth z was determined based on Beer-Lambert's law:

$$I_z = \frac{D_z(UVB)}{10^{\alpha(UVB)\cdot z}} \tag{2}$$

Where $D_z(UVB)$ (J s^{-1} m^{-2}) represents the downwelling irradiance obtained from MeteoSwiss and $\alpha(UVB)$ is the absorbance of the water column of Lake Geneva over the UVB range. For Lake Geneva water, we used an average lake water absorbance $\alpha(320\ nm) = 0.02\ cm^{-1}$ according to measurements (Olive et al., 2020). Values of β_0, β_{temp} and β_{solar} at the surface were taken from the literature (Boehm et al., 2019) whereas solar inactivation beneath the water surface was calculated according to Eq. (2). Table 1 summarizes the β values used in the water quality simulations:

2.3. Sample collection and processing of raw sewage

24-h composite samples of raw sewage were obtained from the Vidy wastewater treatment plant (WWTP) near Lausanne, which collects wastewater of 220′000 inhabitant equivalents. Samples were collected once a month between November 2018 and October 2019. Collected samples were stored at −20 ºC until further processing. Prior to processing, samples were thawed at room temperature. To concentrate the samples, 600 ml aliquots of raw sewage were sequentially filtered through a 2 µm glass fiber pre-filters (cat nº AP2007500, Merck Millipore, Burlington, MA, USA), a 0.45 µm SteriCup filter (cat nº S2HVU02RE, Merck Millipore) and a 0.22 µm SteriCup filter (cat nº SCGVU02RE, Merck Millipore). The filtrate was successively transferred in batches of 50 ml to four different centrifugal filter units with a size cut-off of 100 kDa (Centricon Plus-70; cat nº UFC701008, Merck Millipore) and centrifuged for 30 min at 300×g. After centrifugation, the filtrate was discarded and each centrifugal filter unit was loaded again with 50 ml sample, until the entire 600 ml sample was processed. Finally, the four different centrifugal filters were inverted and centrifuged for 3 min at 1000 ×g to obtain the viral concentrate. Eluted viruses from each centricon unit were pooled and the final volume of the viral concentrate was adjusted to 2 ml by using phosphate-buffered saline (cat nº 18,912,014, Thermofisher Scientific).

Table 1
Beta values applied in the virus inactivation model, taken from Boehm et al. (2019).

Virus type	β_0	β_{temp}	β_{solar} (surface)
Adenovirus	−1.20	0.07	0.13
Enterovirus	−0.25	0.03	1.07
Norovirus	−1.08	0.04	0.43
Rotavirus	−0.60	0.04	0.51

2.4. Nucleic acid extraction and RT-qPCR quantification

Viral nucleic acids (NA) were extracted from 140 µl of viral concentrate by using the Qiagen RNA Viral Mini Kit (cat nº 22,906, Qiagen, Valencia, CA, USA) and the automated QIACube system (Qiagen, Valencia, CA, USA) following the manufacturer's instructions. For each processed batch of sample, a negative extraction control consisting in DNAse/RNAse free molecular water was included. NA were preserved at −80 ºC until further use. Previously published qPCR or RT-qPCR assays were used to quantify the four waterborne viruses of interest, namely human adenovirus (Bofill-Mas et al., 2006; Hernroth et al., 2002), enterovirus (Fout et al., 2016; Monpoeho et al., 2000; Tsai et al., 1993), noroviruses including genogroup GI (Da Silva et al., 2007; Hoehne and Schreier, 2006; Svraka et al., 2007), genogroup GII (Kageyama et al., 2003; Loisy et al., 2005) and genogroup GIV (Miura et al., 2013), and rotavirus (Zeng et al., 2008). Primers and probes used as well as the PCR thermal profiles used are detailed in the supplemental information (Table S1). All amplifications were performed in a final reaction volume of 25 µl and using ten-fold diluted NA viral extracts as a template to minimize inhibition. For adenovirus, master-mixes were prepared using the TaqMan® Environmental Master-Mix 2.0 (Life technologies, Foster City, CA, USA) and 10 µl of ten-fold diluted NA extracts were added as template. For enterovirus, norovirus and rotavirus, master-mixes were prepared using RNA UltraSense™ One-Step Quantitative RT-PCR System (cat nº 11,732–927, Invitrogen, Carlsbad, CA, USA) and 5 µl of ten-fold diluted NA extracts were added as template. All qPCR and RT-qPCR reactions were performed on a Mic qPCR Cycler (Bio Molecular Systems, Upper Coomera, Queensland, Australia). All runs were performed in duplicate and included no-template controls and negative extraction controls to identify any source of contamination during sample processing. In order to provide an absolute quantification of genome copies (GC), qPCR and RT-qPCR standard curves were generated for each viral target using double-stranded DNA gblocks gene fragments at known concentration purchased from Integrated DNA Technologies (Coralville, IA, USA).

2.5. Temporal variations in virus concentrations in sewage

Parametric probability distributions were selected to describe variability and uncertainty in concentrations of each virus species based on monitoring data. We employed two mixed-Poisson distributions, the Poisson lognormal distribution (PLN) and the Poisson gamma distribution (PGA), to describe temporal variations and selected the better fit among the two according to their marginal deviance information criterion (DICm) values (Sylvestre et al., 2021). A difference in DICm of a least 3 points was considered to be significant for model selection. The probability density function of the Poisson lognormal distribution for a random variable x (here the virus count in the sewage sample) is:

$$P_{PLN}(x) = \int_0^{\infty} \frac{(\mu V)^x\ exp(-\mu V)}{x!}\ \frac{1}{\mu s\sqrt{2\pi}} exp\left\{ -\frac{[\ln(\mu) - \zeta]^2}{2s^2} \right\} d\mu \tag{3}$$

where V is the volume of the sample, μ is the mean virus concentration in the sample, ζ is the mean of the logarithm of the virus concentration and

s is the standard deviation of the logarithm of the virus concentration. The probability density function of the Poisson gamma distribution for a random variable x is given by:

$$P_{PGA}(x) = \int_0^{\infty} \frac{(\mu V)^x \, exp(-\mu V)}{x!} \left[\frac{1}{\gamma \Gamma(\delta)} \left(\frac{\mu}{\gamma} \right)^{\delta - 1} exp\left(-\frac{\mu}{\gamma} \right) \right] d\mu \quad (4)$$

where V is the volume of the sample, μ is the mean virus concentration in the sample, and γ and δ are parameters of a gamma distribution which has a mean of $\gamma\delta$ and a variance of $\delta\gamma^2$. Mixed-Poisson distributions were chosen to fit the data as they allow for greater variability in the expected count of the sample than a Poisson distribution with a fixed mean concentration (Haas et al., 2014a).

Bayesian inference was carried out using a Monte Carlo Markov Chain (MCMC) method as described in Sylvestre et al. (2021). Briefly, the priors selected for the lognormal distribution parameters were: a diffuse uniform prior for the mean $\mu_i \sim \mathcal{U}(-10, 10)$ and a vague exponential prior for the standard deviation $\sigma_i \sim \exp(0.1)$. Three Markov chains were run for 10^6 iterations after a burn-in phase of 10^4 iterations. Temporal variations in sewage virus concentrations were illustrated with complementary cumulative distribution functions (CCDF) curves to assess the behavior of the upper tail of these distributions.

2.6. Quantitative Microbial risk assessment (QMRA)

The QMRA process has four main components: hazard identification, exposure assessment, dose-response assessment, and risk characterization (Fewtrell, 2013). Hazard identification serves to determine the pathogen or pathogen group of interest. Here, the hazard is any event or activities that may cause the discharge of virus-contaminated raw sewage into Lake Geneva, such as a heavy rain event. Exposure assessment combines data on the pathogen concentration at the site of interest with information on the rate of intake by an individual, particularly the contact time of lake water to swimmers or direct ingestion of lake water by swimmers. For a conservative estimation, we assumed that 100 ml of virus contaminated water is swallowed by one person during each recreational water event (WHO, 2003). This water intake is high compared to other studies, which have reported that the average water volumes swallowed by adults and children in swimming pools are 16 ml and 37 ml, respectively (Dufour et al., 2006). We addressed the variability of this intake value in one of our simulation cases. The risk characterization is done by integrating the exposure and dose-response models to estimate (per swimming event) negative health outcomes (infection) as a function of the number of viruses ingested. In this study, the exponential dose–response model were employed for enterovirus (Cliver, 1981), beta-Poisson models were applied to adenovirus (Teunis et al., 2016) and rotavirus (Haas et al., 2014b; Ward et al., 1986), and a beta-binomial model was chosen for norovirus (Teunis et al., 2020). Curves of those dose–response models are illustrated in the supplemental information (Fig. S1). The virus dose-response models were originally established using different dose units, whereas viruses in this study were quantified in terms of genome copies (Section 2.4). Therefore, a dose harmonization was conducted to normalize the dose unit of the four types of virus of interest. We followed the dose harmonization rule proposed by McBride et al. (2013). Specifically, we applied the following conversions shown in Table 2:

Monte Carlo stochastic simulations were performed to estimate uncertainties in the computation scheme using R (v4.1.2). We considered uncertainties associated with virus sewage concentration but omitted those associated with water intake volumes. This approach was chosen because the latter uncertainties were not expected to largely affect the relative impact of environmental virus inactivation on health risks, which is the main object of this study. We also did not consider uncertainties associated with dose-response modeling as studies have shown that risks pose by some enteric viruses were insensitive to dose-response parameters (Viau et al., 2011). A total of 10′000 realizations were generated for each type of virus and the uncertainties were computed using a Markov Chain Monte Carlo method.

Table 2
Harmonization factors for viruses investigated in this study, according to McBride et al. (2013).

	Adenovirus	Enterovirus	Norovirus	Rotavirus
Unit used in clinical trials for dose-response relationships	$TCID_{50}$[1]	PFU[2]	GC[3]	FFU[4]
Number of genome copies per clinical trial unit	700	773	1	1900

[1] $TCID_{50}$ = median tissue culture infectious dose.
[2] PFU = plaque forming unit.
[3] GC = genome copies.
[4] FFU = focus-forming units.

2.7. Case studies coupling water quality simulations and QMRA

Using the abovementioned water quality model, we can compute virus concentrations near the shore of Lake Geneva, and when coupled to a QMRA scheme, this reveals the risk of infection. Here we performed case studies to assess the health risks to swimmers at the beach of Morges, a popular summer swimming spot (Fig. 1). Two wastewater treatment plants were considered as the major sources of virus contamination in the Morges region, namely the Vidy WWTP (~8 km east of Morges beach) and the Morges WWTP (~1.5 km east of Morges beach; Fig. 1). Cases were analyzed assuming a failure in the WWTPs, due to technical difficulties, extreme weather or any other possible cause. In such cases, untreated sewage is directly discharged into the surface water via the stormwater outlets near the Vidy WWTP and the Morges WWTP. The sewage discharge was set to 0.7 m^3/s and 5 m^3/s for the Morges WWTP and the Vidy WWTP, respectively, based on their maximum capacities. The water quality model simulated the fate and transport of viruses in this raw sewage after discharge into the lake, for a time span over one week, with three days of continuous release followed by four days of dry period without any discharge of raw wastewater, driven by the actual meteorological conditions observed for periods in 2019 as boundary conditions. Simulations were performed every two weeks per month in 2019, yielding 24 cases in total. The simulation results were then used as pathogen concentrations at the site of interest for the exposure assessment in the QMRA scheme to estimate infection risks to swimmers.

We performed case studies to test four aspects that influence infection risks:

(I) ***Number of contamination sources.*** Two scenarios were considered: in the first, contamination resulted from two simultaneous sources of contamination, the Vidy WWTP and the Morges WWTP, whereas in the second scenario, Vidy WWTP was the only source of contamination. In this case study, we also assessed the influence of intake water volume on the relative risk posed by the four viruses.

(II) ***Different inactivation processes.*** Here, three scenarios of virus inactivation in the lake were simulated: no inactivation (transport only), "background" (β_0) inactivation and "complete" (background, thermal and solar; Eq. (1)) inactivation. For the year of 2019, a summer case from August 18 to 25, and a winter case from December 8 to 15, were analyzed. While not many people swim in the winter, the latter time span was chosen to illustrate the dependence of environmental inactivation processes on season.

(III) ***Variations in virus concentration.*** Stochastic simulations were performed taking the variation of the sewage virus concentration

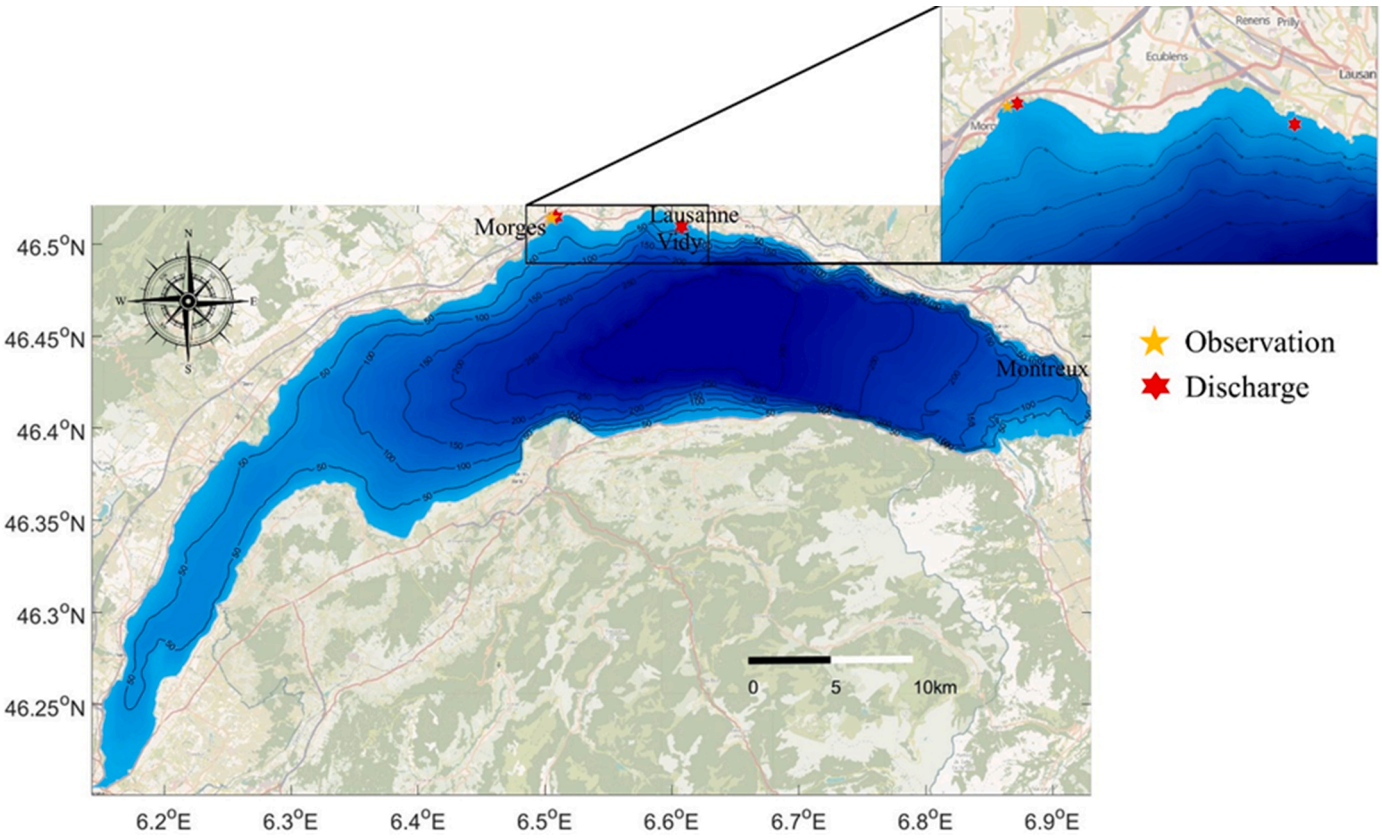

Fig. 1. Map of Lake Geneva with the locations of the virus discharge (Vidy and Morges WWTP) and the observation sites (beach of Morges).

into account. For this case study, the simulation was performed from December 8 to December 15, 2019.

(IV) ***Wind direction.*** The wind condition is one of the most critical factors influencing solute transport near the north shore of Lake Geneva (Bohle-Carbonell, 1991). To determine the role of wind direction for infection risks, results of all 24 simulation cases in 2019 were considered. Wind directions were categorized into two types, the westward wind case which has a mean wind direction of less than 180° during the simulation period, and the eastward wind case, which has a mean wind direction of more than or

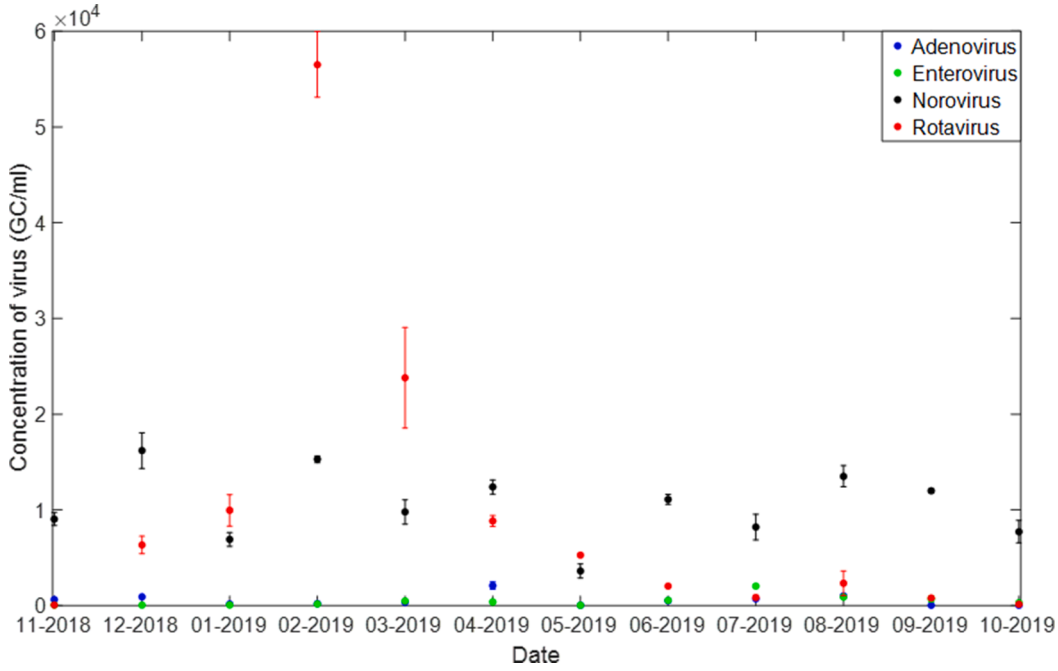

Fig. 2. Monthly measurements of virus concentration in the raw sewage for one year. Bars indicate the values of duplicate PCR measurements. The reported concentrations for norovirus include genogroups GI, GII and GIV.

equal to 180° during the simulation period. This simplified categorization was used to explore the influence of relative wind directions, as our observation site is located almost directly at the west of the discharge sites.

3. Results

3.1. Virus concentrations in raw sewage

The monthly measurements of the enteric viruses considered are illustrated in Fig. 2. Rotavirus reached the highest concentration and peaked in the winter season, while other viruses demonstrated less clear variation patterns according to the limited data set. Adenovirus and enterovirus had concentrations that were on average 1.3 orders of magnitude lower compared with those of rotavirus and norovirus.

For each of the viral species, a Poisson lognormal distribution and a Poisson gamma distribution were employed to fit the measurement data. Because the CCDF curve of empirical data suggested bimodality for rotavirus (Fig. S2), separate fits were performed for the summer (June to November) and winter (December to May) data. Table 3 summarizes the statistics of the PLN and PGA distributions. The CCDF curves, which indicate for each distribution the probability of exceeding a given virus concentration, are shown in Fig. 3.

As seen from Fig. 3, both PLN and PGA distributions fit the observed sewage virus concentrations well. For the DICm calculations, the PLN method gave a slightly smaller deviance than the PGA distribution in general. The PLN distribution for sewage virus concentrations was therefore selected for subsequent analyses. Fitting the rotavirus concentrations with unimodal PGA and PLN distributions resulted in a large uncertainty interval at high concentrations (Fig. S2). The concentration curve shown in Fig. 2 indicated that there was a clear variation over the yearly data for rotavirus that could lead to the bimodal behavior, confirming the need to separate data between summer and winter months.

3.2. Case studies coupling water quality simulations and QMRA

3.2.1. Effect of the number of contamination sources on virus concentration and infection risk

Fig. 4 depicts the concentration of norovirus on August 20 and August 25, 2019, during one simulation from August18 to August 25, 2019, assuming both Vidy and Morges WWTPs are sources of untreated sewage:

As shown in the graphs, the maximum virus concentration at the water surface dropped more than one order of magnitude by August 25 near the shore after the releasing event that ended on August 20. The plume travelled mostly westward to Morges from Vidy Bay, whereas a small portion of the viruses were transported far to the east and reached close to Montreux. The virus concentration and risk levels at the beach site of Morges was then investigated for the same simulation case and for the four types of viruses. Fig. 5 illustrates the change of water quality in terms of virus concentration and infectious risk of the viruses over time, while Fig. S3 demonstrates the results of the same case study yet with a lower water intake volume of only 16 ml per person.

As can be seen from Fig. 5a and c, under the specific environmental conditions during August 18 to August 25, 2019, the influence of the Morges WWTP on the water quality of the beach site at Morges is dominant, despite discharge volume from Morges being substantially lower than the discharge volume from Vidy. The first peak in virus concentration on August 19 is directly linked to the nearby release of the virus contaminated sewage. When only the more distant Vidy WWTP was considered (Fig. 5c), the virus concentrations at the beach of Morges were lower, in particular during the first five days of the simulation though they increased towards the end of the simulation period due to hydrodynamic transport. A longer period of simulation revealed that the influence of this discharge event peaked on August 25 and then rapidly declined (Fig. S4). The infection risks for most of the viruses were up to 100 times (2 logs) lower in the scenario with only one contamination source, apart from norovirus, which remained high even with only one source of contamination (Fig. 5d). This exception for norovirus can be rationalized by the relatively high norovirus concentrations in the sewage, along with the high assumed water intake rate (100 ml intake of lake water in one event) and the dose-response curve of norovirus, which has a much lower 50% infectious dose (82 GC) than the other viruses (799 to $1.4*10^5$ GC; Fig. S1). The risks posed by norovirus would decrease if an average intake value of 16 ml was chosen instead of the highly conservative100 ml (Fig. S3). However, while the risks associated with the other viruses declined almost linearly with the reduction of water intake, the decrease in risks posed by norovirus was only minor, because even at a lower water intake volume the ingested dose was high. Ultimately, the relative risk posed by norovirus compared to the other three viruses was thus larger at low water intake volumes compared to higher ones. Finally, it is worth noting that a higher virus concentration does not always lead to higher infection risk, among different virus types (Fig. 5c and d). Specifically, adenovirus could pose a higher risk than rotavirus even when the concentration of adenovirus was lower.

Table 3
Mean of the measured virus concentrations and the performance indicator (marginal deviance information criterion; DICm) for the Poisson lognormal (PLN) and the Poisson gamma (PGA) distributions.

Parameter/Virus	Adenovirus	Enterovirus	Norovirus	Rotavirus (Summer/Winter)
Mean of samples (GC/ml)	561	482	10,488	1041/18,446
DICm PLN	179	176	253	114/143
DICm PGA	181	183	247	113/178

3.2.2. Contribution of different environmental inactivation processes on virus concentration and infection risk

Figs. 6 and 7 depicts the nearshore virus concentrations (a-d) and the probability of infection risks (e-h) for the four types of viruses included in this study under different inactivation conditions in the summer case and the winter case, respectively.

As the figures indicate, environmental stressors have different impacts on the four virus species studied, depending on the season. For the summer case study, when comparing nearshore virus concentrations resulting from transport alone (red traces in Fig. 6) to those resulting from both transport and environmental inactivation (blue traces), it is evident that environmental inactivation affected enterovirus and rotavirus concentrations to a greater extent than norovirus. However, even norovirus concentrations were lowered by more than 60% due to environmental inactivation when all stressors were included, compared to the concentration arising from transport alone (Fig. 6c). The relative contributions of the different environmental inactivation processes also varied between viruses. As revealed in Fig. 6a–d, thermal and solar inactivation contributed ~35% of the total inactivation rate averaged from the results of the four types of viruses, whereas background inactivation contributed ~65%. Yet, the contribution of solar and thermal inactivation was much higher for adenovirus (62%) and norovirus (51%) than for enterovirus (5%) and rotavirus (23%), whose inactivation were dominated by background inactivation. The influence of environmental stressors on the infection risks therefore also differed between virus species (Fig. 6e,f). At the end of the simulation, background and solar inactivation combined could reduce the infection risk by about three orders of magnitude for enterovirus on August 25 (Fig. 6f, difference between red and blue trace), whereas for norovirus the environmental stressors only reduced the risk level by 15% compared to the cases where only transport was considered.

However, the situation in the winter case study revealed some different characteristics compared with the summer case simulations. First, it is noticeable that, in the winter case, simulations with a

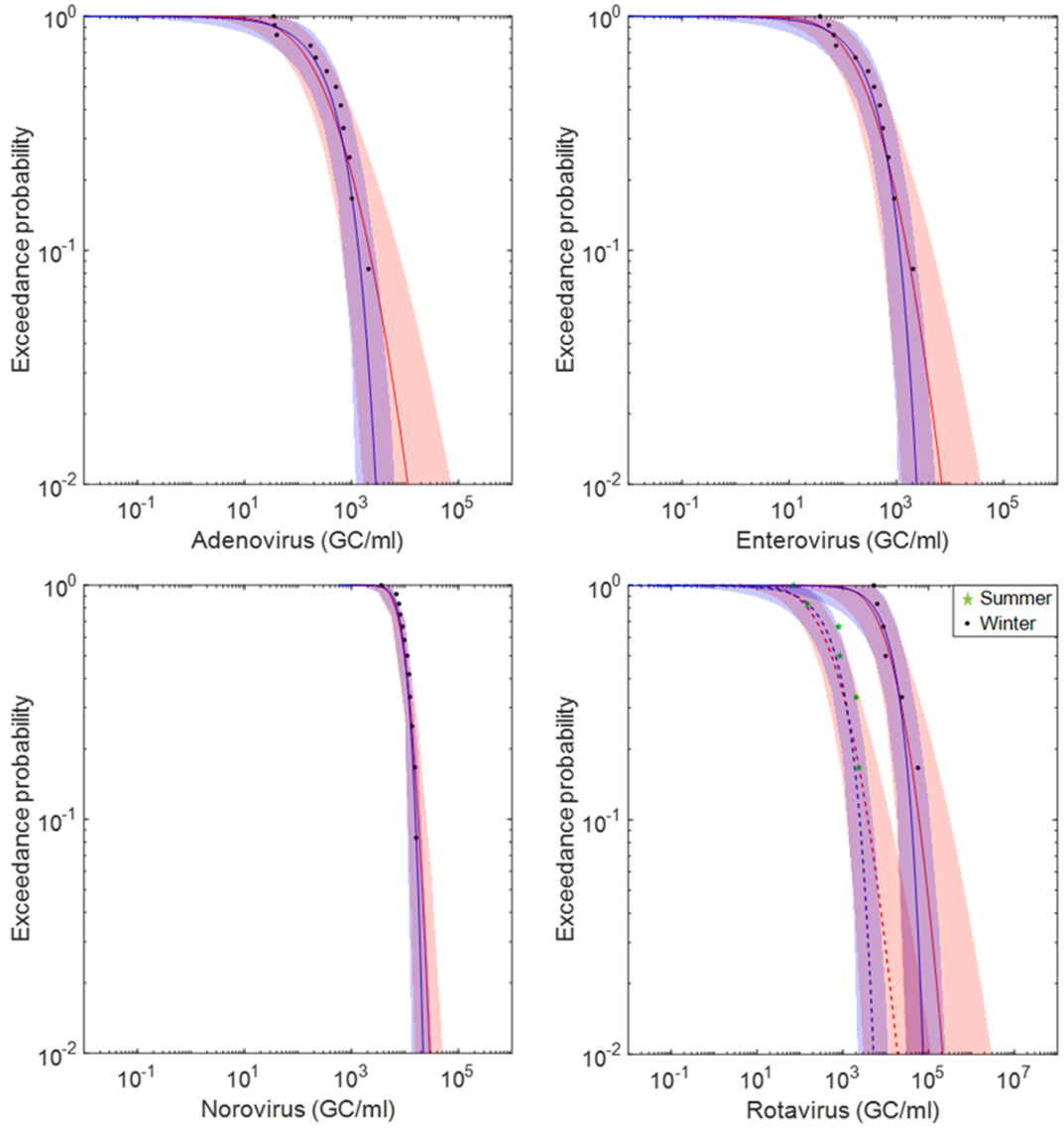

Fig. 3. CCDF graphs of PLN (red) and PGA (blue) distributions for the four different viruses. Black dots and green stars are measurements, shaded areas of the respective color represent the 95% uncertainty interval. In the bottom right panel, rotavirus summer data was shown in green stars and dashed lines while winter data was shown in black dots and solid lines.

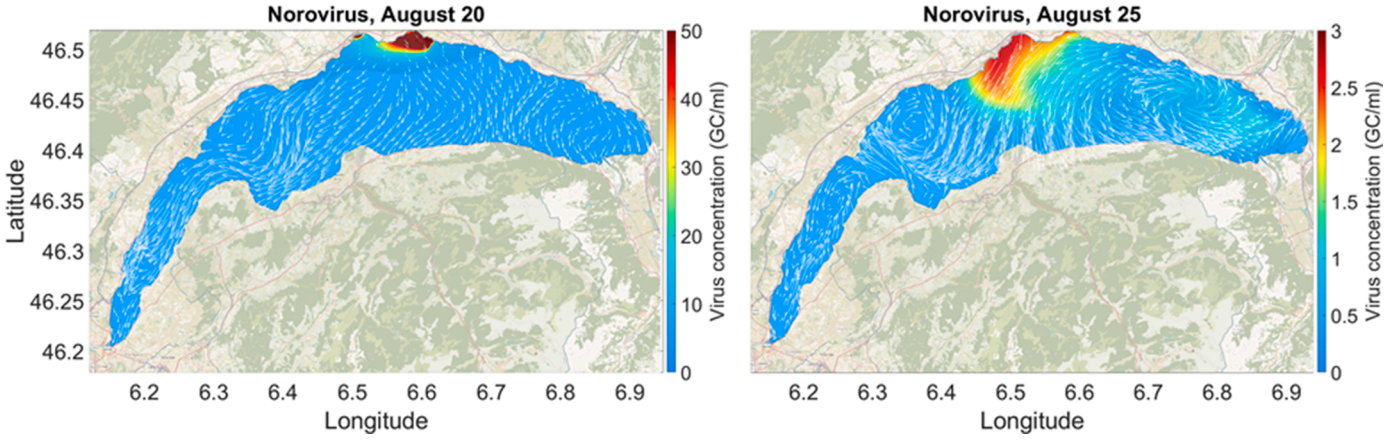

Fig. 4. Simulated surface concentration of norovirus on August 20 and August 25, 2019. The number of viruses released was determined based on virus concentration measurements in August 2019 (Fig. 2). For ease of visualization, virus inactivation and dilution are both represented as a reduction in GC/ml, even though some environmental inactivation processes may reduce virus infectivity via damage to the viral protein capsid rather than genome degradation, and would thus not necessarily manifest as a reduction in GC/ml.

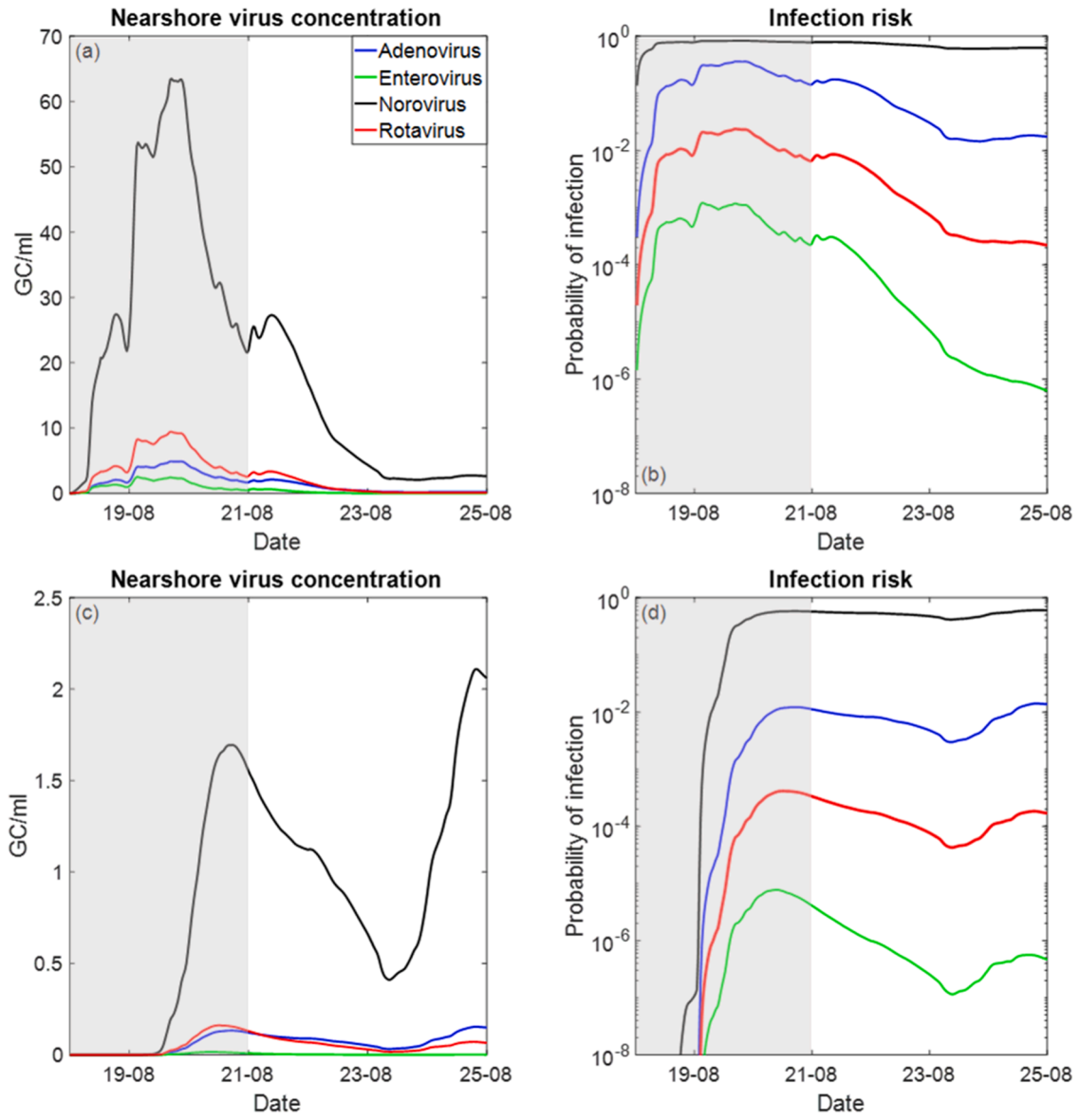

Fig. 5. Nearshore virus concentration and infection risk per swimming event of the viruses based on virus concentration measurements in August 2019. Panels a and b illustrate the results from the scenario with two contamination sources (Vidy and Morges WWTPs), while panels c and d show the results from the scenario with only one source (Vidy WWTP). Gray shade indicates the time when virus contaminated raw sewage was discharged.

"complete inactivation" (blue traces) yielded a higher virus concentration and risks compared with the simulations considering only the "background inactivation" (black traces). This result is associated with the fact that the "background inactivation" was defined for a constant reference temperature of 15 ºC. The actual water temperature in winter, however, is below 15 ºC. The rate constant for "complete inactivation", which includes temperature effects, is therefore lower than that of the "background" scenario. Second, peak nearshore virus concentrations under the specific conditions of the winter scenario were lower than those in the summer scenario. This can be attributed to both differences in the hydrodynamic conditions, as well as the concentrations in sewage (Fig. 2). The combined effect is particularly pronounced for enterovirus, which exhibits lower sewage concentrations in December than in August (Fig. 2), and which therefore exhibited about 20-fold lower nearshore concentrations in the winter. Third, the impact of environmental stressors on the infectious virus concentrations (blue traces) was minor for all viruses. The largest absolute decline in concentration at the end of the simulation period due to virus inactivation was observed for norovirus but corresponded to only 0.18 GC/ml in winter (December 15, panel 7c). In comparison, in the summer scenario the reduction in norovirus concentration at the end of the simulation period was 7.83 GC/ml (August 25, panel 6c). On a relative scale, environmental stressors had the greatest effect on enterovirus followed by rotavirus, similar to what was observed in summer. And finally, consistent with lower virus concentrations, the mean infections risk for all the four viruses were also slightly lower for the winter case compared with the summer case, in particular for enterovirus. The differences between the risks obtained from transport alone (red trace) and those including complete virus inactivation (blue trace) were also much smaller in winter, with the largest difference at around only 1 log at the end of the simulation for enterovirus (December 15, panel 7f).

3.2.3. Variability in infection risk due to variations in virus concentration in sewage

As was discussed above, virus concentrations in sewage are subject to some variation (Fig. 2), and this variation can be modeled by a Poisson lognormal distribution (Fig. 3). Fig. 8 depicts how variations in virus concentrations can influence the infection risk at the Morges beach,

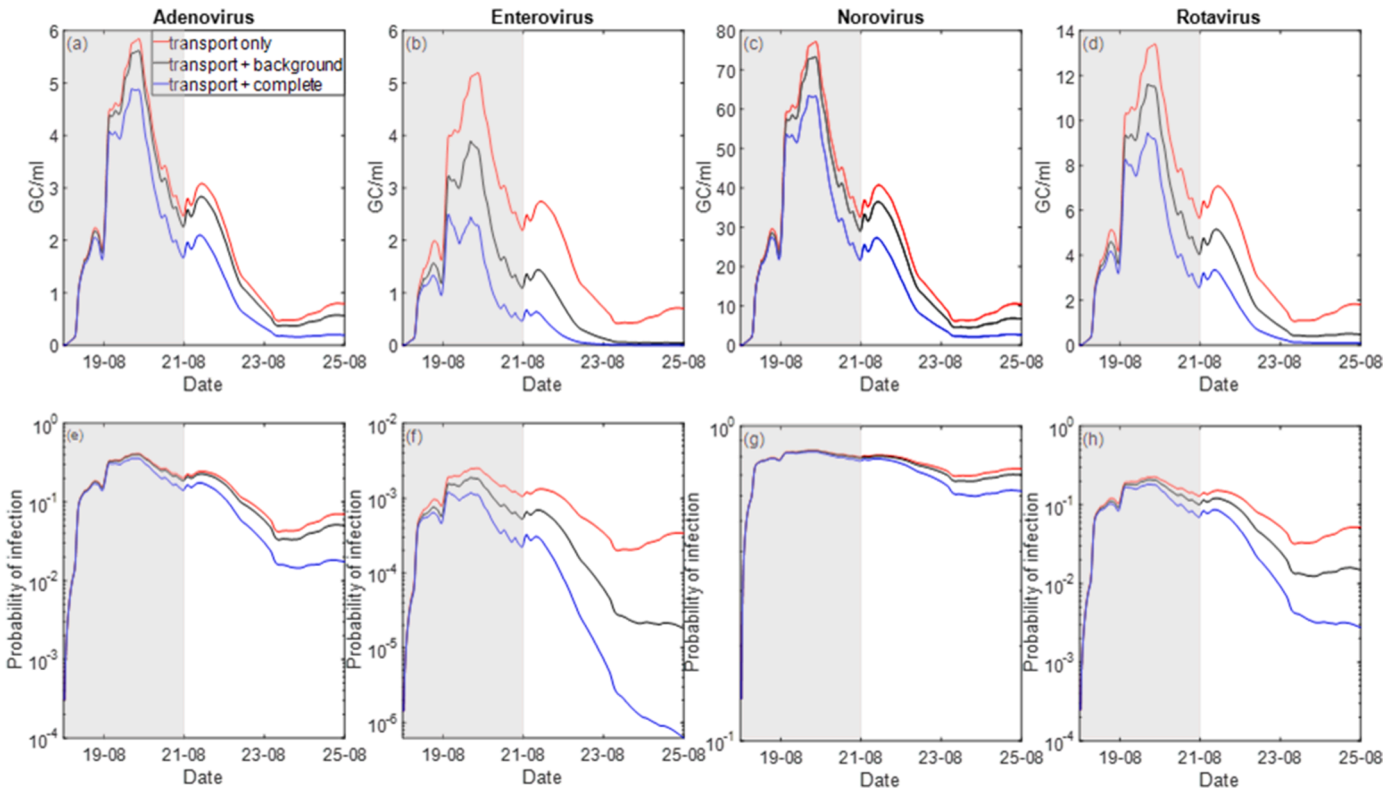

Fig. 6. Nearshore virus concentration of adenovirus (a), enterovirus (b), norovirus (c), rotavirus(d) and their infection risks per swimming event (e-h) under different inactivation situations from August 18 to 25, based on virus concentration measurements in August 2019. "Background" refers to inactivation under reference conditions (in darkness at 15 ℃) and "Complete" means inactivation under real conditions of sunlight and temperature. Gray shade indicates the time when virus contaminated raw sewage was discharged. Note the difference in y-axis scales among the viral species.

using a stochastic simulation performed for December 2019. Here the results are based on the best fit parameterization of the PLN distribution for each enteric virus type. The effect of the parametric uncertainty of the PLN distribution is illustrated in the supplemental file (Figs. S5 and S6). The inclusion of parametric uncertainty gives a wider range in the possible risk values; however, the variability in the virus concentration is still the dominant factor in determining the shape of the risk curves.

As depicted in the graphs, the infection risk of norovirus remained the highest among the virus species considered, while enterovirus had the lowest risk levels. Among the four viruses studied, adenovirus had the largest range of probabilities of infection per swimming event, which spanned from below 10^{-4} to around 10^{0}. This large range can be attributed to the comparatively high variance in the concentrations of adenovirus in the raw sewage.

3.2.4. Influence of wind direction on infection risks

Simulations were carried out twice per month for all of 2019, and the resulting risk levels at the Morges beach are summarized in Table 4, categorized by wind conditions. We emphasize that the simulated risk levels are conservative, given the high water intake volume of 100 ml used.

Norovirus had the highest mean event risk throughout the year, whereas enterovirus had the lowest infection risk, which was more than three orders of magnitude smaller than that of norovirus. Under eastward wind conditions, the infection risks of all viruses were noticeably lower than that under westward wind conditions, except for norovirus, which was acute under both wind conditions. On average, the infection risks under eastward wind conditions were 43% lower than that under westward wind conditions.

4. Discussion

In this work, we coupled measured virus concentrations in sewage, virus transport, virus inactivation and QMRA models to investigate the fate of waterborne viruses from their release at pipe outlets to the risks they pose to human at recreational water sites. Among the viruses studied, it was demonstrated that norovirus had the highest annual mean risk, while the mean risk exerted by enterovirus was several orders of magnitude lower (Table 4). This finding is aligned with previous studies indicating that norovirus causes the highest risks among many commonly found enteric viruses (Soller et al., 2010; Vergara et al., 2016). Adenovirus and rotavirus had similar annual mean risks, which were also at least one order lower than that of norovirus. The measurements of sewage virus concentration indicated possible seasonality for the enteric viruses, especially for rotavirus. Two simple parametric distributions, the PLN and PGA distributions were able to fit the virus measurement data well. These mixed distributions provide alternatives for studies concerning characterization of wastewater virus concentrations using simple component distributions, which typically rely on Weibull (Verani et al., 2019; Vergara et al., 2016) or lognormal distributions (Sunger et al., 2019) to describe pathogen concentrations. We found that physical distance from the contamination source and meteorological parameters (e.g., irradiance, wind) as well as season were essential factors affecting infection risks, and that the inclusion of environmental inactivation in risk assessments could lead to substantially lower risk estimates compared to transport processes alone. The case studies highlighted the importance of combining water quality simulations and QMRA for the study of fate and transport of waterborne viruses near recreational water sites in lakes. Such significance is, needless to say, not confined in the scope of recreational sites in lakes, but also confirmed by studies dedicated to drinking water systems (Sokolova et al., 2015) and rivers and catchments (Schijven et al., 2015).

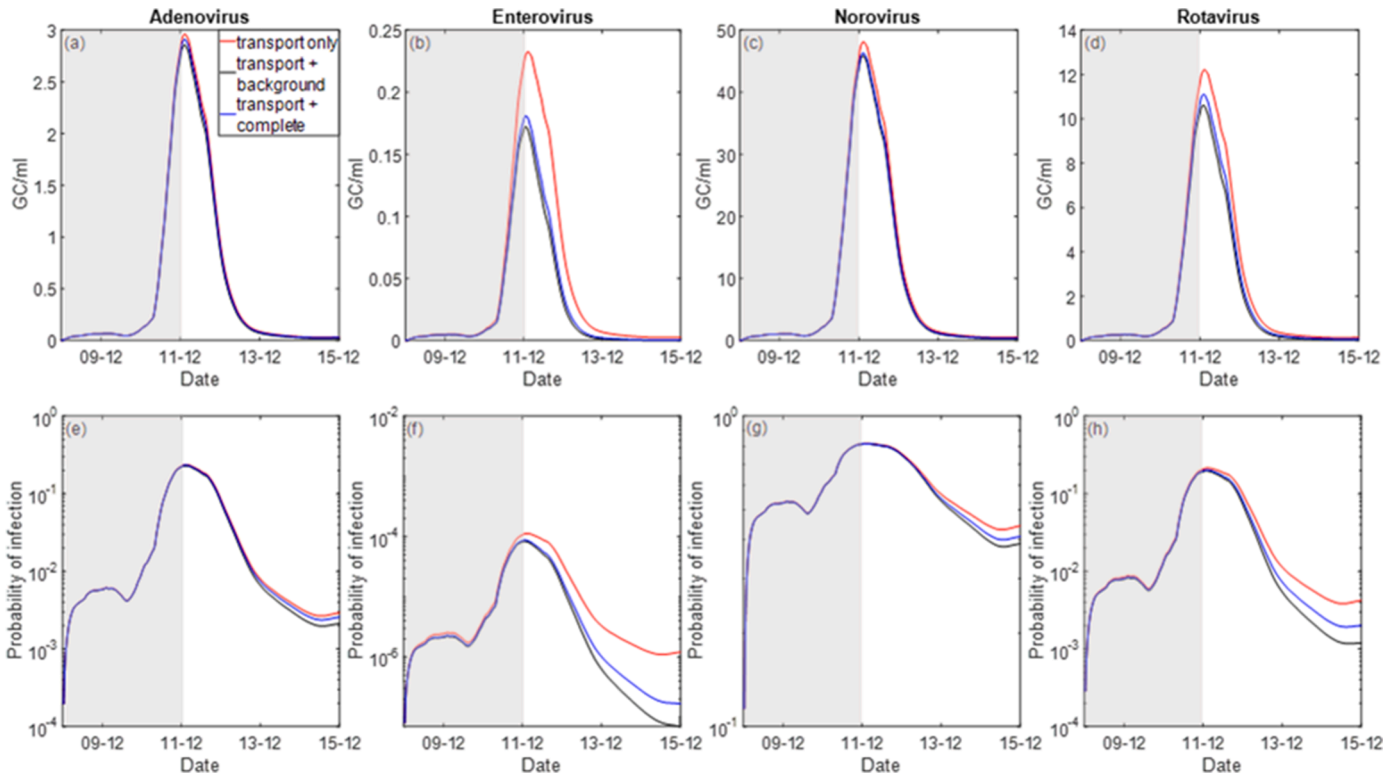

Fig. 7. Nearshore virus concentration of adenovirus (a), enterovirus (b), norovirus (c), rotavirus(d) and their infection risks per swimming event (e-h) under different inactivation situations from December 8 to 15, based on virus concentration measurements in December 2019. "Background" refers to inactivation under reference conditions (in darkness at 15 ℃) and "Complete" means inactivation under real conditions of sunlight and temperature. Gray shade indicates the time when virus contaminated raw sewage was discharged. Note the difference in y-axis scales among the viral species.

4.1. The distance to the contamination sources has direct influence on the risk

Intuitively, the relative distance to contamination site is likely a critical factor influencing the concentration levels and resulting infection risks at the observation site of interest. This has been well confirmed by our simulation of two contamination sources that are either distant (Vidy WWTP) or close (Morges WWTP) to the beach of interest (Fig. 5). The maximum virus concentration was more than 30 times lower if contamination stemmed only from the distant site (Vidy WWTP) compared with the scenario with contributions from both sites. Even though the discharge rate at the Vidy WWTP was much larger than that at Morges WWTP (5 m^3/s versus 0.7 m^3/s), the major contamination at the beach of Morges was triggered by the discharge at Morges WWTP. The lake water between Vidy Bay and the Morges beach site thus served as a buffer area and diluted the virus plume to a large extent. However, while the infection risks of adenovirus, enterovirus and rotavirus dropped significantly if only one contamination site was considered, that of norovirus did not experience much reduction compared with the case with both sources. This highlights the exceptionally infectious nature of norovirus even at small concentrations, which is also related to the exceptionally acute dose-response relationship.

Another important aspect controlling the risk level was the time elapsed since the contamination event, which has been mentioned in many other studies. Boehm et al. (2018) demonstrated that aging of contamination can largely affect the resultant risks, and Wu et al. (2020) indicated that lack of information on the contamination age impedes reliable estimation of the health risk. Taking adenovirus as an example, in the week-long simulation case with two sources, the maximum risk reached 0.35 whereas three days later this risk level was below 0.016. If an individual were informed of such virus releasing events and the transport dynamics, one may plan recreational water activities accordingly and avert the risk of being infected by adenovirus by more than 20-fold (1.3 log). Coupling hydrodynamics and environmental decay alleviates the challenge of not knowing the age of a contamination plume, which is particularly problematic when water quality is assessed based on indicators.

4.2. Environmental stressors noticeably reduce the infection probability exerted by viruses with low background inactivation in summer, but effects in the winter are minor

Adding on the effect of transport and dilution, which are critical factors in many cases, environmental inactivation further lowered the infection risk, in particular during the summer and in most pronounced fashion for enterovirus. However, different viruses underwent very different levels of inactivation and the contribution of different environmental stressors also varied between virus species and seasons. For the summer, on average, the fraction of inactivation by solar and thermal stressors was much greater for adenovirus and norovirus than for enterovirus and rotavirus (Fig. 6). This can be explained by the lower background inactivation rate of adenovirus and norovirus, combined with comparatively high thermal inactivation coefficients (Table 1). Correspondingly, the reduction of infection risks was also significantly different among viruses. Risk reduction due to environmental inactivation was up to three orders of magnitude larger for enterovirus than for adenovirus and norovirus. For the winter, however, the effect of environmental stressors on virus inactivation was less pronounced than in the summer. The "background" simulation, which assumes a reference water temperature of 15 ℃, showed a reduction in virus concentration compared to transport alone (Fig. 7). This reduction is also evident in the "complete" scenario, which accounted for the actual water temperature encountered in winter. However, compared to the "background" simulation, the effect of environmental stressors was smaller, reflecting the

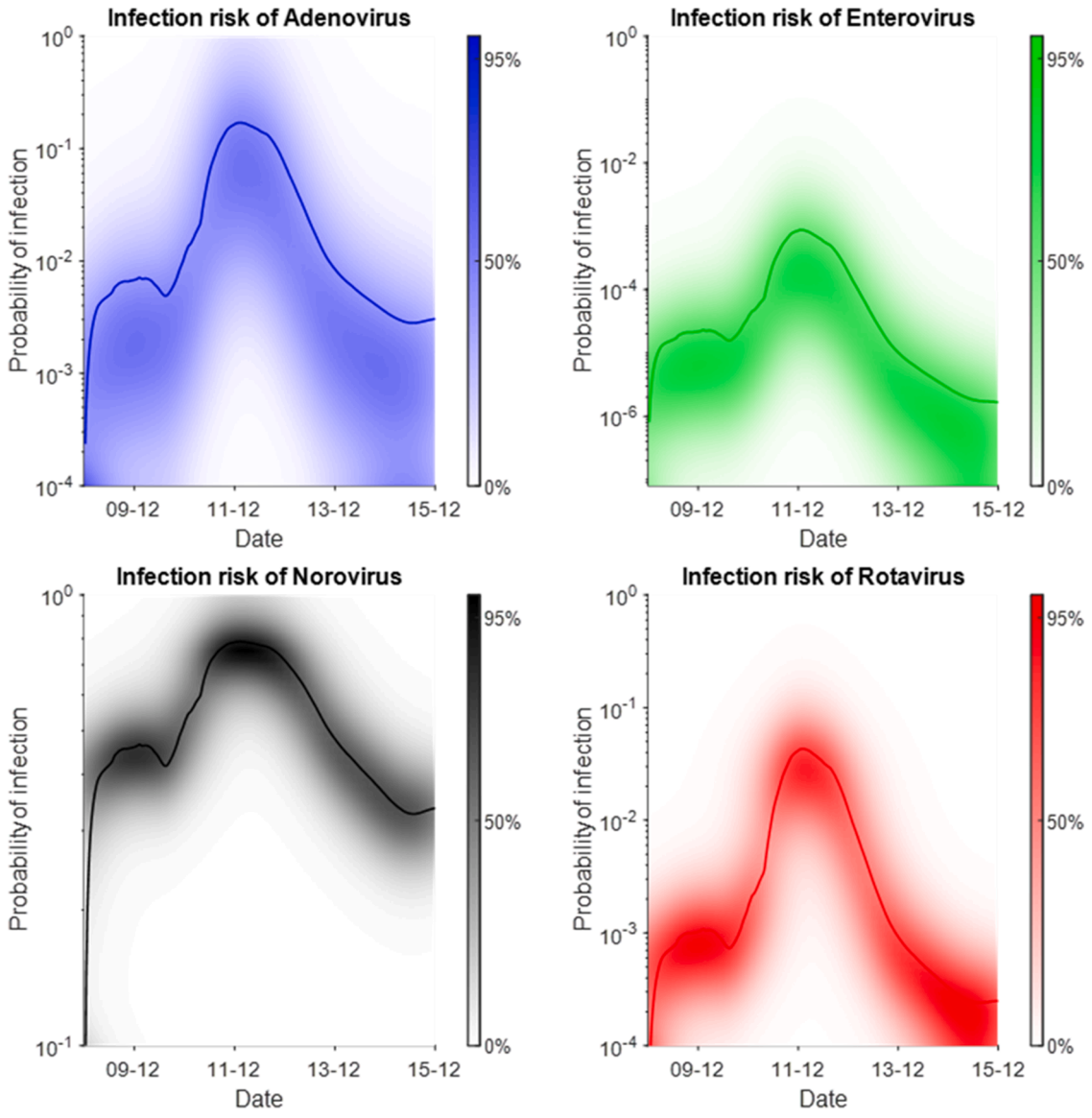

Fig. 8. Stochastic simulation of the infection risks per swimming event at the Morges beach in December 2019. Sewage concentrations were simulated stochastically using the PLN distribution. The solid lines are mean risk values and the shading indicates the frequency of occurrence. For rotavirus the winter season CCDF was used to generate the stochastic simulations.

Table 4
Risk per swimming event averaged over all the simulation cases with statistics of the mean and the standard error.

	Annual mean	Westward wind	Eastward wind
Adenovirus	0.08 ± 0.01	0.09 ± 0.01	0.05 ± 0.01
Enterovirus	0.0003 ± 0.00003	0.0003 ± 0.00003	0.0001 ± 0.00003
Norovirus	0.69 ± 0.02	0.71 ± 0.01	0.60 ± 0.05
Rotavirus	0.04 ± 0.007	0.04 ± 0.009	0.02 ± 0.005

fact that environmental stressors are less effective at inactivating viruses at low temperatures. The results in winter also imply that inactivation due to solar radiation was relatively weak, as the reduction of inactivation due to low temperature outweighed the increase of inactivation brought about by winter solar radiation. The minor contribution of radiation on virus inactivation in cold seasons was also reported in studies concerning infectious hematopoietic necrosis virus by Foreman et al. (2015). These case studies indicate that combining comprehensive water quality simulation and QMRA is necessary in dealing with risk evaluation for waterborne virus transport processes in natural water bodies, with the necessity of specific consideration for different types of viruses and seasonality.

4.3. *Infection probability depends on dominant wind direction*

By summarizing the 24 simulation cases in 2019, the annual risk characterization permits a statistical analysis on the risk levels and some essential factors affecting the risks, such as wind fields. Since the beach site of Morges is located west of both the Vidy Bay and the Morges WWTP, an eastward wind would favor the lower concentrations at the observation site. The risks under eastward wind conditions were noticeably lower than that under westward wind conditions. Take norovirus as an example, under persistent eastward wind conditions, the contamination plume could travel as far east as to the Rhône River inlet, while under strong westward winds, even though the plume did not reach the Rhône River outlet at Geneva, the contaminant was observed in the "Petit Lac" (the small western part) of Lake Geneva (SI Fig. S7). These results highlight the importance of the impact of hydrodynamic transport on virus concentrations, as well as the unrivalled power of water quality models in offering an inclusive prediction of the fate and

transport of virus in lakes, which was also addressed in infectious hematopoietic necrosis virus transport studies for coastal regions (Foreman et al., 2015).

4.4. Limitations and outlook

The framework proposed in our study expands the scope of coupled water quality and risk models to viruses in lakes, however, several limitations remain. Firstly, only background, temperature-driven and solar inactivation of virus were considered in our study, while other factors may also contribute to virus removal from the water column. For instance, the model could be expanded to include virus adsorption to particles and subsequent settling processes, which has been mostly addressed in wastewater treatment rather than in natural water bodies (Templeton et al., 2008), once field studies provide sufficient data to parameterize this process. Secondly, model validation is challenging. It is difficult to conduct sampling campaigns for virus concentration measurements at recreational sites because infectious virus concentration is often low and only a fraction of viruses circulating in the environment can be quantified by available culturing systems. It is also not possible to overcome this limitation by performing spike-in experiments with human virus in the field, due to biosafety considerations. A field measurement campaign to validate the model would have gone beyond the scope of this work but is envisioned for future applications of the model. Thirdly, the current parameterization of environmental virus inactivation is based on an integrated data set across water bodies and virus strains. For higher simulation accuracy, site-and viral strain-specific parameterization would be beneficial. Finally, the QMRA could be further refined. Specifically, our data set of sewage virus concentrations was too small to rigorously capture seasonality trends. To improve the results and reduce the uncertainties in an intuitive way, more data of the sewage virus concentration measurement would be favorable. In addition, we used single scenario values for the water intake volume, the dose-response curves and dose harmonization factors. In reality, however, these values are variables and scenario-dependent. For example, Schets et al. (2011) found that the water intake volume was dependent on gender, age and where the swimming activities take place. Furthermore, dose-response curves vary depending on assumptions regarding the susceptibility of the hosts (Messner et al., 2014) or aggregation of the virus (Van Abel et al., 2017). And finally, the dose-harmonization was found to be dependent on virus species as well as the culturing method applied (Jonsson et al., 2008). To incorporate these uncertainties together with our study could further consolidate the risk assessment for waterborne virus in lakes.

5. Conclusions

This study proposes a coupled water quality and risk model to assess the fate of waterborne viruses from their release to the environment to the associated risks they pose to human at a recreational water site. Our case studies indicate that both transport and environmental inactivation processes are essential in determining the virus concentration at a site of interest. Furthermore, the incorporation of spatially and temporally varying inactivation processes in water quality models is important for evaluating the infection risks. The relative significance of transport and environmental stressors on the infection risks were demonstrated to be highly dependent on the season, meteorological conditions, wind direction and the virus type of concern. Environmental stressors tend to enhance virus inactivation in summer, whereas in winter the effects are in part attenuated by colder water temperatures. Averaged over a year, the infection risks with a mean wind direction that is blowing from the observation site towards the discharge location were 43% lower than that under the reverse condition for the site of concern in this study. The results further showed that norovirus was the most problematic virus species among the four viruses studied and posed a risk that was usually at least one order of magnitude greater than that posed by the other viruses. However, as one example showed, with an informed assessment of the water quality near the beach and an enlightened plan to carry out recreational water activities, one may avert the risk of infection by waterborne virus by more than 20-folds only by delaying the timing of water related activities for three days.

Despite certain limitations, this study serves as one of the first endeavors to integrate virus concentration measurement, virus transport and spatiotemporally varying inactivation simulation as well as QMRA for risk evaluation of waterborne viruses at recreational water sites. The model proposed here can be relatively easily refined and adapted for other locations and employed for comprehensive analysis and prediction of the fate and transport of waterborne viruses in the future.

Declaration of Competing Interest

The authors declare that they have no known competing financial interests or personal relationships that could have appeared to influence the work reported in this paper.

Data availability

Data (measured virus concentrations) and code (data fitting with the simple parametric distributions, parameterization of the distributions, hydrodynamic, water quality and QMRA model setup and boundary conditions) are availabe at https://doi.org/10.5281/zenodo.7386773.

Acknowledgments

This work was supported by the Swiss National Science Foundation (grant no. 31003A_182468). X.F.-C. was a fellow of the European Union's Horizon 2020 research and innovation program under the Marie Skłodowska–Curie Grant Agreement No. 754462. We thank Prof. Alfred Wüest and Dr. Mark Borchardt for their valuable inputs to this work.

Supplementary materials

Supplementary material associated with this article can be found, in the online version, at doi:10.1016/j.watres.2022.119437.

References

Aslan, A., Xagoraraki, I., Simmons, F.J., Rose, J.B., Dorevitch, S., 2011. Occurrence of adenovirus and other enteric viruses in limited-contact freshwater recreational areas and bathing waters. J. Appl. Microbiol. 111, 1250–1261. https://doi.org/10.1111/j.1365-2672.2011.05130.x.

Baracchini, T., Hummel, S., Verlaan, M., Cimatoribus, A., Wüest, A., Bouffard, D., 2020a. An automated calibration framework and open source tools for 3D lake hydrodynamic models. Environ. Model. Softw. 134, 104787 https://doi.org/10.1016/j.envsoft.2020.104787.

Baracchini, T., Wüest, A., Bouffard, D., 2020b. Meteolakes: an operational online three-dimensional forecasting platform for lake hydrodynamics. Water Res. 172, 115529 https://doi.org/10.1016/j.watres.2020.115529.

Boehm, A.B., Ashbolt, N.J., Colford, J.M., Dunbar, L.E., Fleming, L.E., Gold, M.A., Hansel, J.A., Hunter, P.R., Ichida, A.M., McGee, C.D., Soller, J.A., Weisberg, S.B., 2009. A sea change ahead for recreational water quality criteria. J. Water Health 7, 9–20. https://doi.org/10.2166/wh.2009.122.

Boehm, A.B., Graham, K.E., Jennings, W.C., 2018. Can we swim yet? Systematic review, meta-analysis, and risk assessment of aging sewage in surface waters. Environ. Sci. Technol. 52, 9634–9645. https://doi.org/10.1021/acs.est.8b01948.

Boehm, A.B., Silverman, A.I., Schriewer, A., Goodwin, K., 2019. Systematic review and meta-analysis of decay rates of waterborne mammalian viruses and coliphages in surface waters. Water Res. 164, 114898 https://doi.org/10.1016/j.watres.2019.114898.

Bofill-Mas, S., Albinana-Gimenez, N., Clemente-Casares, P., Hundesa, A., Rodriguez-Manzano, J., Allard, A., Calvo, M., Girones, R., 2006. Quantification and stability of human adenoviruses and polyomavirus JCPyV in wastewater matrices. Appl. Environ. Microbiol. 72, 7894–7896. https://doi.org/10.1128/AEM.00965-06.

Bohle-Carbonell, M., 1991. Wind and currents: response patterns of Lake Geneva. Ann. Geophys. 9, 82–90.

Brouwer, A.F., Masters, N.B., Eisenberg, J.N.S., 2018. Quantitative microbial risk assessment and infectious disease transmission modeling of waterborne enteric

pathogens. Curr. Environ. Health Rep. 5, 293–304. https://doi.org/10.1007/s40572-018-0196-x.
Cabelli, V.J., 1983. Public health and water quality significance of viral diseases transmitted by drinking water and recreational water. Water Sci. Technol. 15, 1–15. https://doi.org/10.2166/wst.1983.0036.
Cliver, D.O., 1981. Experimental infection by waterborne enteroviruses. J. Food Prot. 44, 861–865. https://doi.org/10.4315/0362-028x-44.11.861.
Corsi, S.R., Borchardt, M.A., Carvin, R.B., Burch, T.R., Spencer, S.K., Lutz, M.A., McDermott, C.M., Busse, K.M., Kleinheinz, G.T., Feng, X., Zhu, J., 2016. Human and bovine viruses and bacteria at three great lakes beaches: environmental variable associations and health risk. Environ. Sci. Technol. 50, 987–995. https://doi.org/10.1021/acs.est.5b04372.
Da Silva, A.K., Le Saux, J.C.C., Parnaudeau, S., Pommepuy, M., Elimelech, M., Le Guyader, F.S., 2007. Evaluation of removal of noroviruses during wastewater treatment, using real-time reverse transcription-PCR: different behaviors of genogroups I and II. Appl. Environ. Microbiol. 73, 7891–7897. https://doi.org/10.1128/AEM.01428-07.
Deltares, 2015. Delft3D-Flow. User Man. 712.
Dufour, A.P., Evans, O., Behymer, T.D., Cantú, R., 2006. Water ingestion during swimming activities in a pool: a pilot study. J. Water Health 4, 425–430.
Eregno, F.E., Tryland, I., Tjomsland, T., Myrmel, M., Robertson, L., Heistad, A., 2016. Quantitative microbial risk assessment combined with hydrodynamic modelling to estimate the public health risk associated with bathing after rainfall events. Sci. Total Environ. 548–549, 270–279. https://doi.org/10.1016/j.scitotenv.2016.01.034.
Farkas, K., Mannion, F., Hillary, L.S., Malham, S.K., Walker, D.I., 2020. Emerging technologies for the rapid detection of enteric viruses in the aquatic environment. Curr. Opin. Environ. Sci. Health 16, 1–6. https://doi.org/10.1016/j.coesh.2020.01.007.
Fewtrell, L., 2013. Water quality: guidelines, standards and health: assessment of risk and risk management for water-related infectious disease. Water Intell. Online 12. https://doi.org/10.2166/9781780405889.
Foreman, M.G.G., Guo, M., Garver, K.A., Stucchi, D., Chandler, P., Wan, D., Morrison, J., Tuele, D., 2015. Modelling infectious hematopoietic necrosis virus dispersion from marine salmon farms in the Discovery Islands, British Columbia, Canada. PLoS ONE 10, 1–25. https://doi.org/10.1371/journal.pone.0130951.
Fout, G.S., Cashdollar, J.L., Griffin, S.M., Brinkman, N.E., Varughese, E.A., Parshionikar, S.U., 2016. EPA Method 1615. measurement of enterovirus and norovirus occurrence in water by culture and RT-qPCR. Part III. Virus detection by RT-qPCR. J. Vis. Exp. 107, e52646. https://doi.org/10.3791/52646.
Gholipour, S., Ghalhari, M.R., Nikaeen, M., Rabbani, D., Pakzad, P., Miranzadeh, M.B., 2022. Occurrence of viruses in sewage sludge: a systematic review. Sci. Total Environ. 824, 153886 https://doi.org/10.1016/j.scitotenv.2022.153886.
Haas, C.N., Rose, J.B., Gerba, C.P., 2014a. Exposure assessment. Quantitative Microbial Risk Assessment. Wiley Online Books. John Wiley & Sons, Inc, Hoboken, New Jersey, pp. 159–234. https://doi.org/10.1002/9781118910030.ch6.
Haas, C.N., Rose, J.B., Gerba, C.P., 2014b. Conducting the dose-response assessment. Quantitative Microbial Risk Assessment. Wiley Online Books. John Wiley & Sons, Inc, Hoboken, New Jersey, pp. 267–321. https://doi.org/10.1002/9781118910030.ch8.
Hamza, I.A., Jurzik, L., Überla, K., Wilhelm, M., 2011. Methods to detect infectious human enteric viruses in environmental water samples. Int. J. Hyg. Environ. Health 214, 424–436. https://doi.org/10.1016/j.ijheh.2011.07.014.
Hernroth, B.E., Conden-Hansson, A.C., Rehnstam-Holm, A.-S., Girones, R., Allard, A.K., 2002. Environmental factors influencing human viral pathogens and their potential indicator organisms in the blue mussel, Mytilus edulis : the first Scandinavian report. Appl. Environ. Microbiol. 68, 4523–4533. https://doi.org/10.1128/AEM.68.9.4523-4533.2002.
Hipsey, M.R., Antenucci, J.P., Brookes, J.D., 2008. A generic, process-based model of microbial pollution in aquatic systems. Water Resour. Res. 44, 1–26. https://doi.org/10.1029/2007WR006395.
Hipsey, M.R., Antenucci, J.P., Brookes, J.D., Burch, M.D., Regel, R.H., Linden, L., 2004. A three dimensional model of cryptosporidium dynamics in lakes and reservoirs: a new tool for risk management. Int. J. River Basin Manag. 2, 181–197. https://doi.org/10.1080/15715124.2004.9635231.
Hoehne, M., Schreier, E., 2006. Detection of norovirus genogroup I and II by multiplex real-time RT-PCR using a 3′-minor groove binder-DNA probe. BMC Infect. Dis. 6, 69. https://doi.org/10.1186/1471-2334-6-69.
Jonsson, N., Gullberg, M., Lindberg, A.M., 2008. Real-time polymerase chain reaction as a rapid and efficient alternative to estimation of picornavirus titers by tissue culture infectious dose 50% or plaque forming units. Microbiol. Immunol. 53, 149–154. https://doi.org/10.1111/j.1348-0421.2008.00107.x.
Kageyama, T., Kojima, S., Shinohara, M., Uchida, K., Fukushi, S., Hoshino, F.B., Takeda, N., Katayama, K., 2003. Broadly reactive and highly sensitive assay for norwalk-like viruses based on real-time quantitative reverse transcription-PCR. J. Clin. Microbiol. 41, 1548–1557. https://doi.org/10.1128/JCM.41.4.1548-1557.2003.
Li, C., Odermatt, D., Bouffard, D., Wüest, A., Kohn, T., 2022. Coupling remote sensing and particle tracking to estimate trajectories in large water bodies. Int. J. Appl. Earth Obs. Geoinf. 110, 102809 https://doi.org/10.1016/j.jag.2022.102809.
Lodder, W.J., De Roda Husman, A.M., 2005. Presence of noroviruses and other enteric viruses in sewage and surface waters in The Netherlands. Appl. Environ. Microbiol. 71, 1453–1461. https://doi.org/10.1128/AEM.71.3.1453-1461.2005.
Loisy, F., Atmar, R.L.L., Guillon, P., Le Cann, P., Pommepuy, M., Le Guyader, F.S.S., 2005. Real-time RT-PCR for norovirus screening in shellfish. J. Virol. Methods 123, 1–7. https://doi.org/10.1016/j.jviromet.2004.08.023.
McBride, G.B., Stott, R., Miller, W., Bambic, D., Wuertz, S., 2013. Discharge-based QMRA for estimation of public health risks from exposure to stormwater-borne pathogens in recreational waters in the United States. Water Res. 47, 5282–5297. https://doi.org/10.1016/j.watres.2013.06.001.
McLaughlin, A.J., 1912. The prevention of water-borne disease in lake and river traffic. Boston Med. Surg. J. 167, 831–834. https://doi.org/10.1056/NEJM191212121672402.
Messner, M.J., Berger, P., Nappier, S.P., 2014. Fractional poisson - A simple dose-response model for human norovirus. Risk Anal. 34, 1820–1829. https://doi.org/10.1111/risa.12207.
Miura, T., Parnaudeau, S., Grodzki, M., Okabe, S., Atmar, R.L., Le Guyader, F.S.F.S., 2013. Environmental detection of genogroup I, II, and IV noroviruses by using a generic real-time reverse transcription-PCR assay. Appl. Environ. Microbiol. 79, 6585–6592. https://doi.org/10.1128/AEM.02112-13.
Monpoeho, S., Dehée, A., Mignotte, B., Schwartzbrod, L., Marechal, V., Nicolas, J.C., Billaudel, S., Férré, V., 2000. Quantification of enterovirus RNA in sludge samples using single tube real-time RT-PCR. BioTechniques 29, 88–93. https://doi.org/10.2144/00291st03.
Nelson, K.L., Boehm, A.B., Davies-Colley, R.J., Dodd, M.C., Kohn, T., Linden, K.G., Liu, Y., Maraccini, P.A., McNeill, K., Mitch, W.A., Nguyen, T.H., Parker, K.M., Rodriguez, R.A., Sassoubre, L.M., Silverman, A.I., Wigginton, K.R., Zepp, R.G., 2018. Sunlight-mediated inactivation of health-relevant microorganisms in water: a review of mechanisms and modeling approaches. Environ. Sci. Process. Impacts 20, 1089–1122. https://doi.org/10.1039/c8em00047f.
Olive, M., Gan, C., Carratalà, A., Kohn, T., 2020. Control of waterborne human viruses by indigenous bacteria and protists is influenced by temperature, virus type, and microbial species. Appl. Environ. Microbiol. 86, e01992. https://doi.org/10.1128/AEM.01992-19. -19.
Rigosi, A., Hanson, P., Hamilton, D.P., Hipsey, M., Rusak, J.A., Bois, J., Sparber, K., Chorus, I., Watkinson, A.J., Qin, B., Kim, B., Brookes, J.D., 2015. Determining the probability of cyanobacterial blooms: the application of Bayesian networks in multiple lake systems. Ecol. Appl. 25, 186–199. https://doi.org/10.1890/13-1677.1.
Schets, F.M., Schijven, J.F., de Roda Husman, A.M., 2011. Exposure assessment for swimmers in bathing waters and swimming pools. Water Res. 45, 2392–2400. https://doi.org/10.1016/j.watres.2011.01.025.
Schijven, J., Derx, J., de Roda Husman, A.M., Blaschke, A.P., Farnleitner, A.H., 2015. QMRAcatch: microbial quality simulation of water resources including infection risk assessment. J. Environ. Qual. 44, 1491–1502. https://doi.org/10.2134/jeq2015.01.0048.
Searcy, R.T., Taggart, M., Gold, M., Boehm, A.B., 2018. Implementation of an automated beach water quality nowcast system at ten California oceanic beaches. J. Environ. Manag. 223, 633–643. https://doi.org/10.1016/j.jenvman.2018.06.058.
Sinclair, R.G., Jones, E.L., Gerba, C.P., 2009. Viruses in recreational water-borne disease outbreaks: a review. J. Appl. Microbiol. 107, 1769–1780. https://doi.org/10.1111/j.1365-2672.2009.04367.x.
Sokolova, E., Petterson, S.R., Dienus, O., Nyström, F., Lindgren, P.-E., Pettersson, T.J.R., 2015. Microbial risk assessment of drinking water based on hydrodynamic modelling of pathogen concentrations in source water. Sci. Total Environ. 526, 177–186. https://doi.org/10.1016/j.scitotenv.2015.04.040.
Soller, J.A., Bartrand, T., Ashbolt, N.J., Ravenscroft, J., Wade, T.J., 2010. Estimating the primary etiologic agents in recreational freshwaters impacted by human sources of faecal contamination. Water Res. 44, 4736–4747. https://doi.org/10.1016/j.watres.2010.07.064.
Sunger, N., Hamilton, K.A., Morgan, P.M., Haas, C.N., 2019. Comparison of pathogen-derived 'total risk' with indicator-based correlations for recreational (swimming) exposure. Environ. Sci. Pollut. Res. 26, 30614–30624. https://doi.org/10.1007/s11356-018-1881-x.
Svraka, S., Duizer, E., Vennema, H., de Bruin, E., van der Veer, B., Dorresteijn, B., Koopmans, M., 2007. Etiological role of viruses in outbreaks of acute gastroenteritis in The Netherlands from 1994 through 2005. J. Clin. Microbiol. 45, 1389–1394. https://doi.org/10.1128/JCM.02305-06.
Sylvestre, É., Prévost, M., Smeets, P., Medema, G., Burnet, J.-B., Cantin, P., Villion, M., Robert, C., Dorner, S., 2021. Importance of distributional forms for the assessment of protozoan pathogens concentrations in drinking-water sources. Risk Anal. 41, 1396–1412. https://doi.org/10.1111/risa.13613.
Templeton, M.R., Andrews, R.C., Hofmann, R., 2008. Particle-associated viruses in water: impacts on disinfection processes. Crit. Rev. Environ. Sci. Technol. 38, 137–164. https://doi.org/10.1080/10643380601174764.
Teunis, P., Schijven, J., Rutjes, S., 2016. A generalized dose-response relationship for adenovirus infection and illness by exposure pathway. Epidemiol. Infect. 144, 3461–3473. https://doi.org/10.1017/S0950268816001862.
Teunis, P.F.M., Le Guyader, F.S., Liu, P., Ollivier, J., Moe, C.L., 2020. Noroviruses are highly infectious but there is strong variation in host susceptibility and virus pathogenicity. Epidemics 32, 100401. https://doi.org/10.1016/j.epidem.2020.100401.
Tolouei, S., Dewey, R., Snodgrass, W.J., Edge, T.A., Andrews, R.C., Taghipour, M., Prévost, M., Dorner, S., 2019. Assessing microbial risk through event-based pathogen loading and hydrodynamic modelling. Sci. Total Environ. 693, 133567 https://doi.org/10.1016/j.scitotenv.2019.07.373.
Tong, H.I., Connell, C., Boehm, A.B., Lu, Y., 2011. Effective detection of human noroviruses in Hawaiian waters using enhanced RT-PCR methods. Water Res. 45, 5837–5848. https://doi.org/10.1016/j.watres.2011.08.030.
Trung Thanh, H., Tschakert, P., Hipsey, M.R., 2021. Moving up or going under? Differential livelihood trajectories in coastal communities in Vietnam. World Dev. 138, 105219 https://doi.org/10.1016/j.worlddev.2020.105219.

Tsai, Y.L., Sobsey, M.D., Sangermano, L.R., Palmer, C.J., 1993. Simple method of concentrating enteroviruses and hepatitis A virus from sewage and ocean water for rapid detection by reverse transcriptase-polymerase chain reaction. Appl. Environ. Microbiol. 59, 3488–3491. https://doi.org/10.1128/aem.59.10.3488-3491.1993.

Van Abel, N., Schoen, M.E., Kissel, J.C., Meschke, J.S., 2017. Comparison of risk predicted by multiple norovirus dose–response models and implications for quantitative microbial risk assessment. Risk Anal. 37, 245–264. https://doi.org/10.1111/risa.12616.

Verani, M., Federigi, I., Donzelli, G., Cioni, L., Carducci, A., 2019. Human adenoviruses as waterborne index pathogens and their use for Quantitative Microbial Risk Assessment. Sci. Total Environ. 651, 1469–1475. https://doi.org/10.1016/j.scitotenv.2018.09.295.

Vergara, G.G.R.V., Rose, J.B., Gin, K.Y.H., 2016. Risk assessment of noroviruses and human adenoviruses in recreational surface waters. Water Res. 103, 276–282. https://doi.org/10.1016/j.watres.2016.07.048.

Viau, E.J., Lee, D., Boehm, A.B., 2011. Swimmer risk of gastrointestinal illness from exposure to tropical coastal waters impacted by terrestrial dry-weather runoff. Environ. Sci. Technol. 45, 7158–7165. https://doi.org/10.1021/es200984b.

Ward, R.L., Bernstein, D.I., Young, E.C., Sherwood, J.R., Knowlton, D.R., Schiff, G.M., 1986. Human rotavirus studies in volunteers: determination of infectious dose and serological response to infection. J. Infect. Dis. 154, 871–880. https://doi.org/10.1093/infdis/154.5.871.

WHO, 2021. Guidelines on Recreational Water quality. Volume 1, Coastal and Fresh Waters. World Health Organization, 2021.

WHO, 2011. Guidelines for Drinking-Water Quality, 38. WHO chronicle, pp. 104–108.

WHO, 2003. Guidelines for Safe Recreational Water environments. Volume 1, Coastal and Fresh Waters. World Health Organization, 2003.

WHO Scientific Group, 1979. Human Viruses in water, Wastewater and soil : WHO Technical Report Series. World Health Organization. No. 639 (1979).

Wong, M., Kumar, L., Jenkins, T.M., Xagoraraki, I., Phanikumar, M.S., Rose, J.B., 2009. Evaluation of public health risks at recreational beaches in Lake Michigan via detection of enteric viruses and a human-specific bacteriological marker. Water Res. 43, 1137–1149. https://doi.org/10.1016/j.watres.2008.11.051.

Wu, B., Wang, C., Zhang, C., Sadowsky, M.J., Dzakpasu, M., Wang, X.C., 2020. Source-associated gastroenteritis risk from swimming exposure to aging fecal pathogens. Environ. Sci. Technol. 54, 921–929. https://doi.org/10.1021/acs.est.9b01188.

Zeng, S.-.Q., Halkosalo, A., Salminen, M., Szakal, E.D., Puustinen, L., Vesikari, T., 2008. One-step quantitative RT-PCR for the detection of rotavirus in acute gastroenteritis. J. Virol. Methods 153, 238–240. https://doi.org/10.1016/j.jviromet.2008.08.004.